A Force Field for Phosphoric Acid: Comparison of Simulated with Experimental Data in the Solid and Liquid State

Stéphane A. H. Spieser,*,† Bas R. Leeflang,‡ Loes M. J. Kroon-Batenburg,† and Jan Kroon†

Department of Crystal & Structural Chemistry, and Department of Bio-Organic Chemistry, Bijvoet Center for Biomolecular Research, Utrecht University, Padualaan 8, 3584 CH Utrecht, The Netherlands

Received: January 12, 2000; In Final Form: May 4, 2000

A force field for phosphoric acid is developed, on the basis of the reproduction of the experimental crystal structure by molecular dynamics (MD) simulations. The fit between calculated and experimental unit cell parameters, atomic positions, thermal motions, and hydrogen bond distances is satisfactory. Subsequently, MD simulations in the liquid state are carried out. Simulated and experimental liquid properties, in particular the diffusion coefficient and the radial pair distribution functions, show again good agreement, which can be seen as a validation of our parametrization.

Introduction

Phosphoric acid has long been the subject of theoretical studies,[1−4] incited by the role played by phosphates in biological systems. The acid itself has also many industrial applications: metal treatment (rust protection), chemical polishing, food industry applications,[5] production[6−9] of fibers from anisotropic solutions with cellulose. Highly concentrated phosphoric acid (HCPA) is a complex system. As a function of concentration, polymerization occurs and a distribution of molecular species is present in solution[10] {orthophosphoric acid (H_3PO_4), pyrophosphoric acid ($H_4P_2O_7$), and polyphosphoric acid [$H(PO_3H)_n$-OH $n > 2$]}. HCPA can be considered as hydrated phosphorus pentoxide (P_2O_5). H_3PO_4 (100% w/w) is P_2O_5 in the fully hydrated state (water free) and corresponds to 72.4% P_2O_5 (w/w). At this particular concentration, however, ca. 15% of the phosphorus atoms belong to the dimer species.[11]

To our knowledge, no force field has been described in the literature for phosphoric acid. In the framework of our study on the interactions of cellulose and phosphoric acid, it is of great importance to investigate the conformational influence of phosphoric acid on cellulose structure, at the molecular level, to improve our understanding of the mechanical properties of the derived fibers. The goal of this study is to set up a force field for phosphoric acid that will be used as an explicit solvent system in molecular dynamics (MD) simulations of carbohydrates.

Methods

Force Field. In molecular mechanics calculations as well as in MD simulations, the interactions between molecules are described by a nonbonded potential U_{NB}. The basic form (eq 1) in the force field we use, GROMOS,[12] is a sum over all atomic pairs of a van der Waals and an electrostatic term,

$$U_{NB} = \sum_i \sum_{j>i} \left[\frac{C_{12}^{(i,j)}}{r_{ij}^{12}} - \frac{C_6^{(i,j)}}{r_{ij}^6} + \frac{q_i q_j}{4\pi\epsilon_0 r_{ij}} \right] \quad (1)$$

in which q_i and q_j are the partial charges, r_{ij} is the distance between the two atoms, and C_{12} and C_6 are the Lennard-Jones parameters. Within a molecule, the bonded potential terms used are,

$$U_b = \sum_i \frac{1}{2} K_b [b - b_0]^2;\ U_\theta = \sum_i \frac{1}{2} K_\theta [\theta - \theta_0]^2;\ U_\Phi = \sum_i K_\Phi [1 + \cos(n\Phi - \delta)] \quad (2)$$

where K_b and K_θ are the force constants and b_0 and θ_0 the equilibrium values of the bond distance and bond angle terms respectively, K_Φ the energy barrier, n the multiplicity, and δ the phase of the torsional term.

MD simulations of crystals provide a good test for the quality of force fields. Indeed, detailed results such as cell parameters, atomic positions (and thermal vibrations), and hydrogen-bond geometries can be compared with accurate experimental data.

The existing parameters for phosphates in GROMOS 87 were first used as an initial trial force field for orthophosphoric acid. However, as will been shown below, the agreement of the resulting unit cell parameters with those of the experimental crystal structure is very poor (Table 1). Thereafter the following iterative process was performed: (1) Modifications in the force field: partial charges, Lennard-Jones parameters, bonded terms; (2) 200-ps MD simulation in NPT ensemble at 300 K and 1 atm; (3) monitoring of unit cell parameters, atomic positions and thermal vibrations, and hydrogen-bond geometries and comparison with experimental crystal structure.

The set of parameters that best reproduces the experimental data is then kept for the rest of the study.

Calculations. All simulations were carried out in the NPT ensemble. Periodic boundary conditions were used. The temperature was kept constant using a weak coupling to a temperature bath[13] of 300 K with a relaxation time of 0.1 ps. The size of the time steps was 1 fs. All bond lengths were allowed to fully relax. Anisotropic (crystal) or isotropic (liquid) pressure scaling was performed at a constant pressure of 1 atm. The compressibility $\beta = 5.7921 \times 10^{-5}$ bar^{-1} was taken over from water, the precise value being unimportant, as it is divided by the adjustable coupling time constant τ_p which, after trials, was taken to be 15 ps. The cutoff radius for the long-range

* Corresponding author.
† Department of Crystal & Structural Chemistry.
‡ Department of Bio-Organic Chemistry.

10.1021/jp000161p CCC: $19.00
Published on Web 07/15/2000

TABLE 1: Unit Cell Parameters[a] in Phosphoric Acid Crystal and from MD Simulations Using Original GROMOS and Our New Force Field (FF)

	original FF	new FF	crystal unit cell
a (Å)	5.192(1)	5.522(2)	5.757(1)
b (Å)	5.037(2)	4.924(2)	4.831(2)
c (Å)	11.300(2)	11.666(2)	11.574(2)
β (degrees)	83.872(40)	94.461(3)	95.274(12)
d (g/cm^3)	2.213	2.058	2.030

[a] Standard deviations in parentheses.

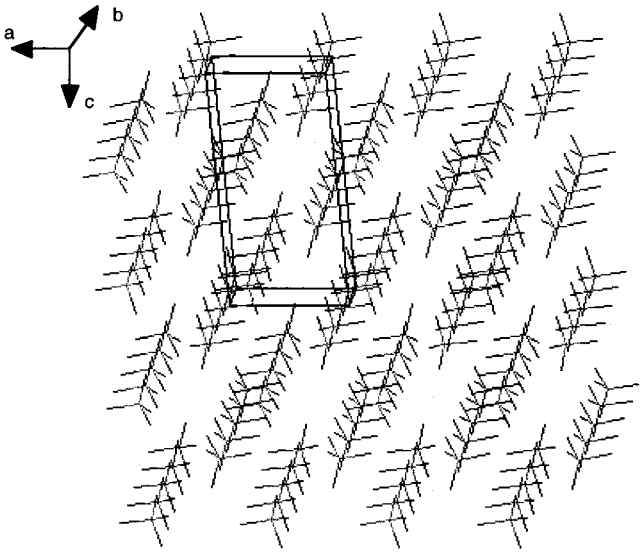

Figure 1. Model system of crystal orthophosphoric acid (hydrogen atoms are omitted for clarity).

interactions was 9 Å using a molecular pair list that was updated every 5 steps. We have used this particular value for the cutoff radius because the carbohydrate force field is optimized with this value and the radial pair distribution of phosphoric acid shows no structure beyond 7−8 Å. Ab initio point charges were derived by fitting to the electrostatic potential at the SCF/6-31G** level of theory using the crystal structure geometry, and applying the programs GAMESS-UK and MOLDEN.[14]

Crystal. Souhassou et al.[15] reported the crystal structure at high-resolution X-ray diffraction of orthophosphoric acid at room temperature, space group $P_{21/c}$. An earlier neutron diffraction analysis[16] was used to model the hydrogen structure of the crystal. The monoclinic simulation box was built up from 4 × 5 × 2 unit cells (160 molecules of orthophosphoric acid) to obtain box dimensions of about 23−24 Å in the three directions (see Figure 1). No symmetry was imposed during the simulations. The first 100 ps of the MD simulation were considered to be the equilibration time. Analysis of the crystal structure simulation is performed by calculating the average box dimensions and the average coordinates and thermal motion by superimposing all orthophosphoric molecules on a reference one by applying space group symmetry operations and translations, averaged over all time steps for the last 200 ps of the trajectory. Coordinates of each frame were corrected for the change of the origin of the system box. Translation parameters were calculated using the program PLATON.[17]

Liquid State. Liquid systems were obtained by heating the crystal structure to 900 K for some hundred picoseconds. When no long-range order was observed anymore, the temperature was gradually decreased to 300 K, in steps of 50 K per 30 ps until 500 K, followed by 25 K per 30 ps. At 300 K, a cubic box of 160 molecules with a length of 24.0349 Å was chosen while maintaining the density and allowed to equilibrate, and a final trajectory of 500 ps was recorded. Physical properties were calculated from this trajectory.

The self-diffusion, $D(t)$, of the phosphoric acid during the MD simulations can be calculated using:

$$D(t) = \frac{\langle |\mathbf{r}_i - r_i(t=0)|^2 \rangle}{6t} \tag{3a}$$

where r_i is the center of mass position of molecule i and t the time during which the position of the molecule is monitored. The average is taken over all molecules and time intervals t. The diffusion coefficient can be obtained from:

$$D = \lim_{t \to \infty} D(t) \tag{3b}$$

Similarly, the radial pair distribution function was calculated from:

$$g_\alpha^\beta(r) = \frac{N_\alpha^\beta(r,\Delta r)}{MN\rho V(r,\Delta r)} \tag{4}$$

where $N_\alpha^\beta(r, \Delta r)$ is the number of β atoms found in a spherical shell of radius r and thickness Δr with respect to a reference α atom, M is the number of time-steps, N is the total number of α atoms, ρ is the number density of β atoms, and $V(r, \Delta r)$ is the volume of a spherical shell of radius r and thickness Δr.

Both properties are compared with experimental values.

NMR Spectroscopy. Diffusion measurements were acquired using a pulsed gradient spin-echo NMR experiment[18] on either a Bruker AMX500 NMR spectrometer (Utrecht university) equipped with a 5-mm proton probe or on a homemade 400-MHz spectrometer (Leiden university) equipped with a 5-mm broadband probehead. The pulse sequence consists of the normal spin-echo experiment with, in addition, identical pulsed field gradients during both half periods before and after the 180° refocusing pulse. The delay between the two gradient pulses determines the time the spin is allowed to diffuse.

$$\ln\left(\frac{I_g}{I_0}\right) = -\left[\gamma^2\delta^2G^2\left(\Delta - \frac{\delta}{3}\right)\right]D \tag{5}$$

With eq 5 it is possible to obtain the self-diffusion constant D, where I_g is the peak integral observed in the presence of the pulsed field gradient, I_0 the peak integral value observed in absence of the pulsed field gradient, γ the gyromagnetic ratio of the observed nucleus, δ (400 μs) the duration of the gradient, Δ (10 ms) the delay between the two gradients, G the variable gradient strength (max. 200 G/cm), and D the diffusion constant. Thus, a plot of $\ln(Ig/I_0)$ versus G^2 yields the diffusion constant from the slope.

Results and Discussion

Force-Field Setup and Crystal Simulations. The challenge of the present study turned out to be the reproduction in the simulation of the short hydrogen bonds present in the crystal structure (distance H−O 1.58−1.62 Å) while maintaining the unit cell parameters close to the experimental values.

Using the original GROMOS force field, the monoclinic angle reduced quickly to ca. 83°, about 10° less than the experimental value (Table 1). The density stabilized around a value of 2.21 g/cm^3, whereas it is 2.03 g/cm^3 in the crystal. Moreover, the hydrogen bond network almost completely lost its initial (crystal structure) arrangement, which is shown in Figure 2.

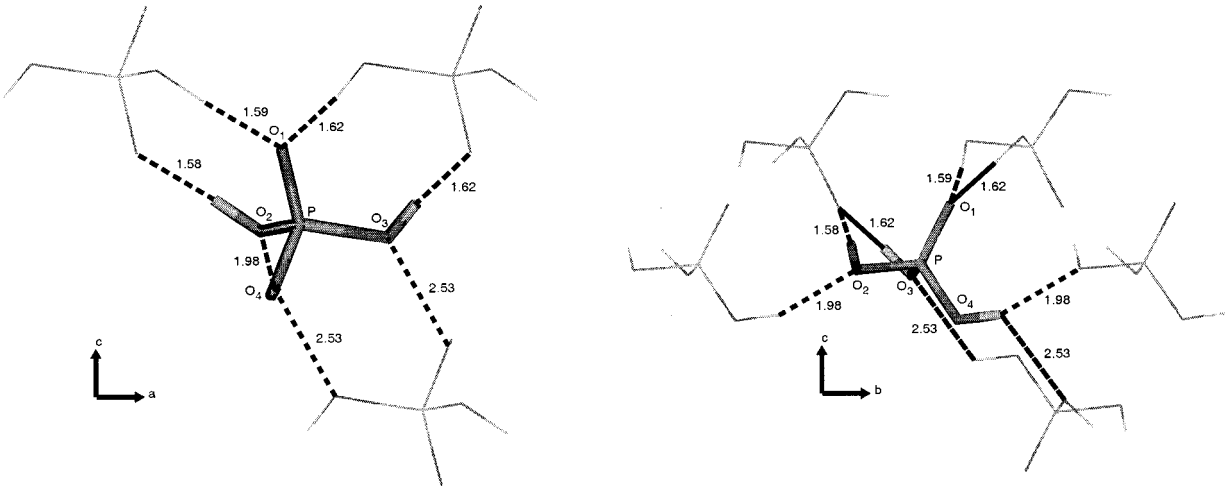

Figure 2. Hydrogen bond network in crystal structure (distances are in angstroms). Left projection on *ac* plane and right projection on *bc* plane.

TABLE 2: Point Charge Sets from Original GROMOS Force Field and Derived from *Ab Initio* Calculations

	q (e) original	*q* (e) ab initio
P	0.83	1.230
O1	−0.38	−0.825
O2,O3,O4	−0.55	−0.600
H2,H3,H4	0.40	0.465

Taking into account the fact that the potential energy function in GROMOS does not contain any specific terms for hydrogen bonds, but focuses only on a good balance between the electrostatic and van der Waals interactions, special attention should be put on these two terms to reproduce the crystal structure accurately.

When point charges derived from ab inito calculations (Table 2) were used, shortening of the hydrogen bonds in the direction of those observed in the crystal structure occurred, but at the expense of a more dense packing of the model system. Furthermore, oscillations in the simulations occurred because of strong intramolecular attractions between oxygen and hydrogen atoms. A systematic search yielded similar charge values. To avoid such strong attractions, 1−4 repulsion on the hydrogen atom [1−4 $C_{12}^{1/2} = 100$ (kcal mol^{-1} Å^{12})$^{1/2}$] was applied. In addition, reduction of the OH bond length and increase of the POH bond angle have been applied to better reproduce the crystal structure values. To improve the density, while having short hydrogen bonds, the steric repulsion on the phosphorus atom was iteratively increased until the unit cell parameters reached a satisfying agreement with the crystal structure. Then the steric repulsion on the double-bonded oxygen was stepwise decreased until the short hydrogen bonds matched well. Finally, fine concerted corrections on both double-bonded oxygen and phosphorus atom repulsion parameters were applied, leading to the results summarized in Table 1. The new force field is presented in Table 3.

Figure 3 shows the trajectories of the unit cell parameters for 300 ps using the final parameter set. Box dimensions equilibrated after a few tens of picoseconds. In Table 1, it is shown that the **a** dimension has the largest deviation (0.23 Å), whereas the two other cell dimensions agree with those of the crystal structure within 0.1 Å. The monoclinic angle, β, is now stable with a deviation less than 1°. Our model is slightly more dense than the crystal structure because of the shrinkage of the **a** dimension. Figure 4 shows the ORTEP representation[16] of the crystal structure and the simulated structure. In both cases the largest motion is observed for the H4 hydrogen atom. It is

TABLE 3: Force Field for Orthophosphoric Acid

bond stretching in kcal/mol/Å^2 and Å:

	K_b	b_0
HO−OA	750.0	0.97
OA−P	600.0	1.61
OM−P	900.0	1.48

angle bending in kcal/mol/rad^2 and degrees:

	K_θ	θ_0
HO−OA-P	95.0	123.0
OA−P−OA	110.0	103.0
OM−P−OA	95.0	109.6

dihedral potential in kcal/mol and degrees:

	K	δ	n
HO−OA−P−O	0.25	0	3
0.75	0	2	

van der Waals (Lennard-Jones 6−12):

	C_6 (kcal/mol Å^6)$^{1/2}$	C_{12} (kcal/mol Å^{12})$^{1/2}$
HO	0.0	100 (1−4)
AO	23.25	600.0
OM	23.25	700.0
P	59.35	5757.0

noticeable that this atom, in the crystal structure, is involved in a bifurcated hydrogen bond (Figure 2). In our simulations, the H4 hydrogen atom is hydrogen-bonded alternatively to O2 or O3. Only ca. 20% of the time the bifurcated hydrogen bond really exists. This means that this hydrogen atom oscillates between two positions, increasing the thermal vibration in that particular direction. In Table 4 the average bond distances and bond angles between atoms involved in hydrogen bonds are listed. A good accordance between the crystal structure and the model system is observed. The discrepancy between the hydrogen bond parameters, calculated using two different approaches, average hydrogen bond distances or hydrogen bond distances from the average structure (vide supra), illustrates the averaging problems.

The agreement between the calculated and the experimental cell parameters and hydrogen bonds is good, but not surprising because the model has been devised to fit these properties. However, there is also a nice agreement of the atomic positions and thermal vibrations.

Liquid State. Figure 5 illustrates the melting process by plotting the system density as a function of time and the imposed temperature. First the crystal structure is heated to 900 K for

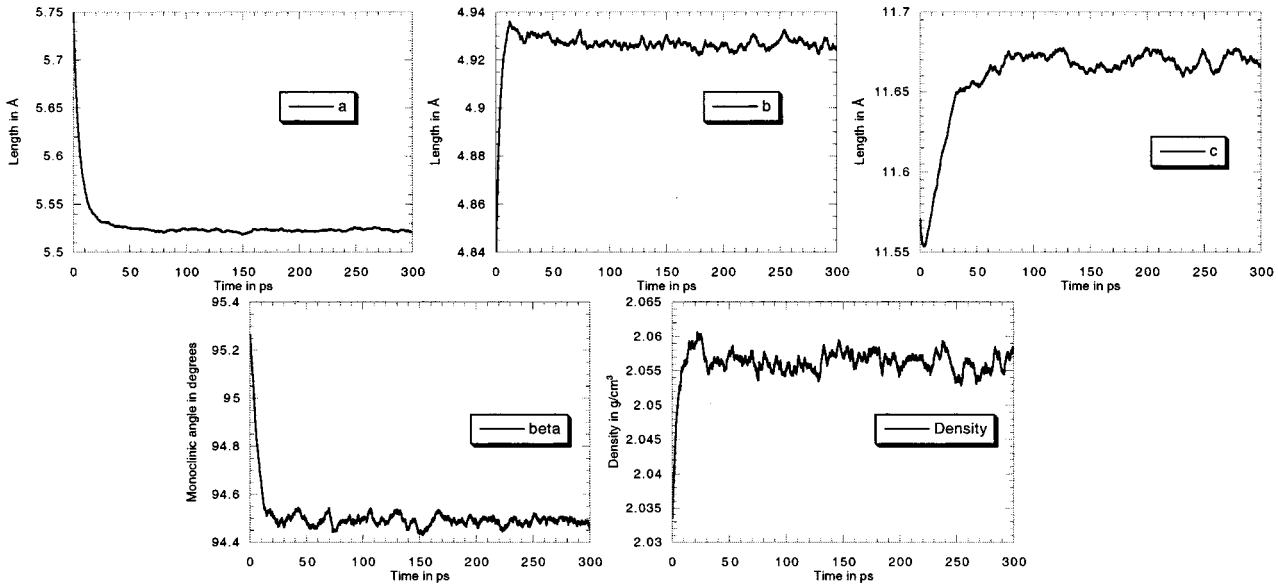

Figure 3. Unit cell parameters and density during 300 ps starting from the crystal structure using the new force field.

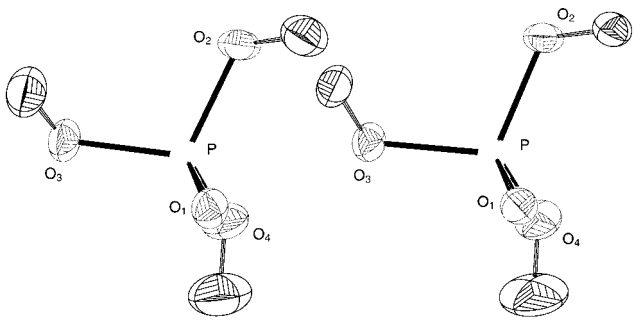

Figure 4. Displacement ellipsoid plots of phosphoric acid molecule showing 50% probability in the crystal structure (left) determined by X-rays[15] and the average structure (see text) of the simulated crystal (right). Plots of the earlier neutron diffraction structure[16] are indistinguishable from this X-ray diffraction structure.

some period to break the order of the crystalline network. This is monitored by calculating the running mean-square displacement of orthophosphoric atoms (not presented), which has to show a linear increase in the liquid state, in contrast with a plateau that is quickly reached with a crystal-like structure. The time needed to break the crystalline order appeared to be 200 ps. The density diminished to 1.58 g/cm^3. Thereafter the system is cooled to room temperature and allowed to equilibrate. The final density of our simulated box, 1.89 g/cm^3, is close to the experimental density[19] of 1.87 g/cm^3, measured at room temperature. Even if the melting temperature of orthophosphoric acid is only at 44.2 °C, because of supercooling properties it is possible to experimentally measure physical properties, like the radial pair distribution function or the diffusion constant, at room temperature.

Experimentally the choice of the phosphoric acid sample is of importance. Below 100% w/w H_3PO_4 content, the sample is not water free. However, at 100% w/w H_3PO_4 the dimeric species, the pyrophosphoric acid, is already present to an amount of 15%. Our calculations do not involve either water molecules or polymeric phosphoric acid species. As our simulated system is 100% orthophosphoric acid, a sample of 93.1% w/w H_3PO_4 (which represents the highest phosphoric acid concentration without polymeric species[11]) was chosen for comparison.

The ^{1}H NMR spectrum of a 93.1% w/w H_3PO_4 solution shows one broad peak ($\Delta\nu_{1/2} = 20$ Hz). The diffusion coefficient determined from ^{1}H NMR measurements at room temperature, using eq 5, gives a value of 9.2×10^{-11} m^2/s. In the literature no experimental values are available in this concentration range. However, a value of 2.5×10^{-11} m^2/s is calculated using the Stokes−Einstein equation, which relates the diffusion coefficient to the viscosity (0.092 Pa s) under the approximation of a spherical shape of the orthophosphoric molecules (radius 2.18675 Å). The discrepancy by a factor of four was quite surprising. We choose then to measure the ^{31}P nucleus too, because a rapid proton exchange rate could be present, which can increase artificially the diffusion rate. The ^{31}P spectrum of a solution of 93.1% w/w H_3PO_4 at room temperature shows one peak, indicating the presence of only the monomeric species. A value of 2.3×10^{-11} m^2/s for the diffusion coefficient was then determined. The agreement between this value and the one derived from the viscosity is now quite good. In contrast, ^{1}H NMR experiments yielded an accurate diffusion coefficient of water.[20] Therefore, the proton exchange rate in phosphoric acid solution must be much higher than in water. From a trajectory of 500 ps, the time-dependent diffusion coefficient was determined using eq 3a (Figure 6). The match between the calculated, 1.1×10^{-11} m^2/s (eq 3b), and the experimental diffusion coefficient is rather good. A slower diffusion in the calculation was expected indeed because in the experiment the presence of water molecules led to an increase of diffusion of the orthophosphoric acid molecules.

The radial pair distribution function, $g(r)$, of phosphoric acid, has recently been determined experimentally at room temperature using neutron diffraction.[21] It gives insight into the structure of the liquid. At that time, only preliminary MD simulations using a crude force field were calculated to guide the interpretation of the experimental data. Figure 7 shows the experimental and our newly calculated $g_{XX}(r)$ and $g_{HX}(r)$ using eq 4, where X means every atom except a H. Both experimental $g_{HX}(r)$ and $g_{XX}(r)$ are the addition of several components. For example, $g_{XX}(r)$ is the weighted sum of $g_{OO}(r)$, $g_{OP}(r)$, and $g_{PP}(r)$. The curves calculated from the MD trajectory have been corrected, using weight factors derived from the experimental measurements. The match between experimental and calculated $g_{XX}(r)$ [$=0.673\ g_{OO}(r) + 0.298\ g_{OP}(r) + 0.033\ g_{PP}(r)$] curves is very good. The first peak at 1.5 Å represents the O−P covalent bond. At the left side of the peak a shoulder is observed

TABLE 4: Average Hydrogen Bond Distances (Å) and Valence Angles (degrees) for Average Structures over 200 ps

	$r_{H\cdots O}$			$r_{O\cdots O}$			$\theta_{O-H\cdots O}$		
	(1)[a]	(2)[b]	crystal	(1)[a]	(2)[b]	crystal	(1)[a]	(2)[b]	crystal
O2−H2···O1	1.59(3)	1.58	1.58	2.57(1)	2.56	2.56	167(2)	175	176
O3−H3···O1	1.622(2)	1.60	1.62	2.591(2)	2.58	2.59	166(1)	173	173
O4−H4···O2	1.935(5)	2.03	1.98	2.824(3)	2.90	2.85	153(1)	157	155
O4−H4···O3	2.322(7)	2.57	2.54	2.899(3)	3.08	3.08	119(2)	115	117

[a] Average distances and angles calculated from MD trajectory. [b] Distances and angles calculated from MD average structure.

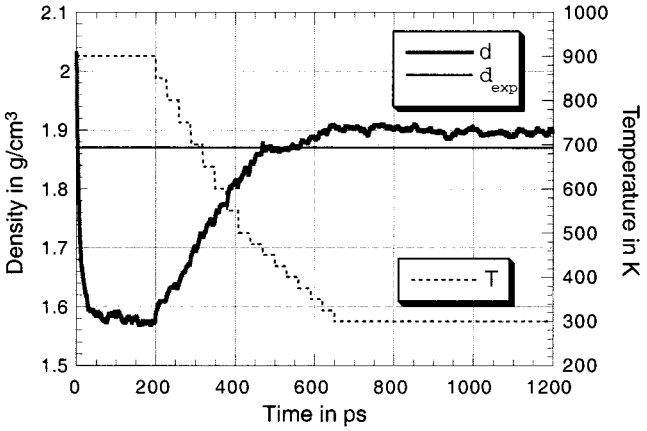

Figure 5. System density as a function of time and by change of temperature.

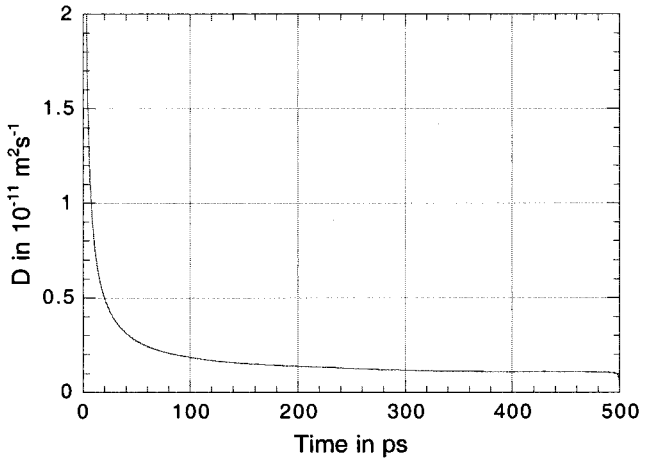

Figure 6. Time-dependent diffusion calculated using eq 3a.

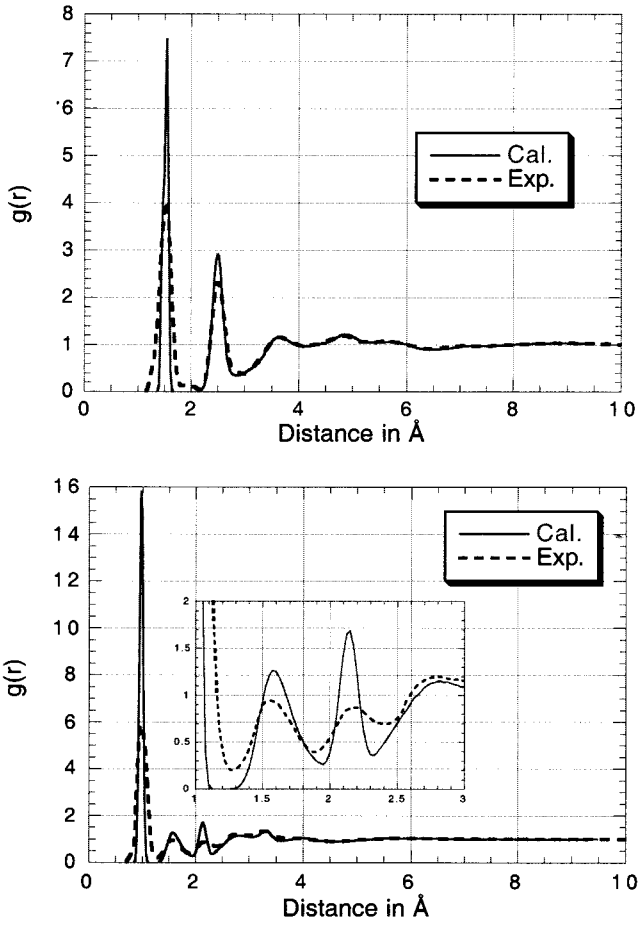

Figure 7. Experimental and calculated radial pair distribution functions; X−X (upper), H−X (lower) with closer view of the hydrogen bond part (inset); X means every atom except an H.

in the experimental curve, which is the consequence of the double-bonded O−P present in the orthophosphoric acid. It seems thus that delocalization does not occur and that the double-bond character is preserved. The difference in peak heights for the covalently bonded atoms is due to the apparently too-large bond length force constant used in our empirical calculations, which strongly restrains the bond lengths close to their equilibrium values. In view of the fact that it is a simple classical force field aimed at describing intermolecular (solvent) interactions, we spent no effort in improving these force constants. Experimentally the coordination number[22] for the covalent O−P bond is 1.16(15). Within the experimental error, each oxygen atom is thus covalently bound to the phosphorus atom. Numerical integration of the same peak in the calculated curve gives a coordination number of 0.97, in agreement with the experiment. The second peak is identified as a mixture of the intramolecular and intermolecular hydrogen-bonded O−O distances. Integration of the peak in the experimental curve gives a coordination number of 3.8(2). With the help of the MD simulations it is straightforward to decompose this peak in its two components, by computing the intramolecular and intermolecular $g_{OO}(r)$. A value of 3.0 is expected for the intramolecular O−O distances in an isolated PO_4 tetrahedron. Coordination numbers, calculated from the MD simulation, of 3.2 and 0.9 are found by numerical integration of the intramolecular and intermolecular O−O radial pair distributions, respectively. The aforementioned difference of ca. 0.8 must therefore be ascribed to intermolecular hydrogen-bonded O atoms at about 2.5 Å. The agreement between the peaks at longer distances demonstrates the good description of long-range order by the force field. The experimental and calculated $g_{HX}(r)$ [=0.823 $g_{HO}(r)$ + 0.182 $g_{HP}(r)$] curves show also good agreement. The first peak represents the H−O covalent bond. The same feature with the too-large bond force constants holds for the coordination number of directly bonding atoms. Experimentally the coordination number is 0.95(10), which is, within error, one oxygen atom directly bonded to a H atom. The second peak corresponds to the H−O distances in hydrogen bonds. The agreement between the simulation (1.57 Å) and the experiment (1.54 Å) is very satisfactory. The coordination number derived

from the peak in the experimental and calculated curves gives 0.75(15) and 0.95 respectively, and fits with the value of 0.8 found for O−O in the $g_{XX}(r)$. The third peak at 2.2 Å is assigned to intramolecular H−P interactions. The fourth peak at 2.8 Å is composed by an overlap of intramolecular H−O (double-bonded oxygen atom) and intermolecular H−P interactions. The fifth peak at 3.25 Å is assigned to H−O intramolecular interactions. It corresponds to an average H−O distance from the three staggered conformations of the H−O−P−O torsion angles. The hydroxyl groups have thus no preferred orientation with respect to neighbor intramolecular oxygen atoms. Further studies are planned to investigate the influence of water content on the liquid-state properties.

Conclusion

In this work, new force-field parameters have been derived for phosphoric acid on the basis of a comparison of the simulated and experimental crystal structure of orthophosphoric acid. The good agreement of density, diffusion coefficient, and radial pair distribution functions shows that our force field is transferrable to the liquid state.

Acknowledgment. This work was supported by The Netherlands Program for Economic Ecology and Technology, #EETK96095, with financial aid of the Ministry of Economic Affairs and the Ministry of Education, Culture and Sciences. We thank Wijnand Mooij for the ab initio determination of the orthophosphoric acid partial charges and the NMR department of Leiden University for providing facilities for the determination of the diffusion coefficient using phosphorus nucleus. GAMESS−UK is a package of ab initio programs written by M. F. Guest, J. H. van Lenthe, J. Kendrick, K. Schoffel, P. Sherwood, and R. J. Harrison, with contributions from R. D. Amos, R. J. Buenker, M. Dupuis, N. C. Handy, I. H.Hillier, P. J. Knowles, V. Bonacic-Koutecky, W. von Niessen, V. R. Saunders, and A. J. Stone. The package is derived from the original GAMESS code due to M. Dupuis, D. Spangler, and J. Wendoloski, NRCC Software Catalog, Vol. 1, Program no. QG01 (GAMESS), 1980.

References and Notes

(1) Moss, G. R.; Souhassou, M.; Blessing, R. H. *Acta Crystallogr.* **1995**, *B51*, 650.
(2) Colvin, M. E.; Evleth, E.; Akacem, Y. *J. Am. Chem. Soc.* **1995**, *117*, 4357.
(3) Ewig, C. S.; van Wazer, J. R. *J. Am. Chem. Soc.* **1985**, *107*, 1965.
(4) O'Keeffe, M.; Domenges, B.; Gibbs, G. V. *J. Phys. Chem.* **1985**, *89*, 2304.
(5) Toy, A. D. F. *Comprehensive Inorganic Chemistry*; Pergamon Press: Elmsford, NY, 1973.
(6) Boerstoel, H.; Koenders, B. M.; Westerink, J. B. WO9606208 (Akzo Nobel).
(7) GB 263810 (British Celanese).
(8) Turbak, A. F.; Hammer, R. B., Davies, R. E.; Hergert, H. L. *Chemtech* **1980**, 51.
(9) Kamide, K.; Miyamoto, I.; Okajima, K. *Polym. J.* **1993**, *25*, 453.
(10) *Ullmann's Encyclopedia of Industrial Chemistry*, 5th ed.; VCH: Weinheim, 1991; Vol. A19.
(11) Jameson, R. F. *J. Chem. Soc.* **1959**, 752.
(12) van Gunsteren, W. F. GROMOS, Groningen molecular simulation package. University of Groningen, 1987.
(13) Berendsen, H. J. C.; Postma, J. P. M.; Gunsteren, W. F.; DiNiola, A.; Haak, J. R. *J. Chem. Phys.* **1984**, *81*, 3684.
(14) Schaftenaar, G. MOLDEN; QCPE−619; QCPE Bulletin Vol. 12, No. 3, 1992.
(15) Souhassou, M.; Espinosa, E.; Lecomte, C.; Blessing, R. H. *Acta Crystallogr.* **1995**, *B51*, 661.
(16) (a) Blessing, R. H. *Acta Crystallogr.* **1988**, *B44*, 334. (b) Blessing, R. H. *Acta Crystallogr.* **1989**, *B45*, 200.
(17) Spek, A. L. PLATON: multipurpose crystallographic program. Utrecht University 1999.
(18) Stilbs, P. *Prog. NMR Spectrosc.* **1987**, *19*, 1.
(19) *Gmelins Handbuch der anorganischen Chemie*, Teil 16C, 8 Aufl; VCG: Weinheim, 1965.
(20) Holz, M.; Weingartner, H. *J. Magn. Reson.* **1991**, *92*, 115.
(21) Tromp, R. H.; Spieser, S. A. H., Neilson, G. W. *J. Chem. Phys.* **1999**, *110*, 2145.
(22) Calculated using eq 9 of ref 21.